Am J Cancer Res 2015;5(5):1751-1761
www.ajcr.us /ISSN:2156-6976/ajcr0006864

Original Article

Inhibition of STAT3 reduces proliferation and invasion in salivary gland adenoid cystic carcinoma

Lin-Lin Bu[1,2], Wei-Wei Deng[1,2], Cong-Fa Huang[1], Bing Liu[2], Wen-Feng Zhang[2], Zhi-Jun Sun[1,2]

[1]The State Key Laboratory Breeding Base of Basic Science of Stomatology & Key Laboratory of Oral Biomedicine Ministry of Education, School & Hospital of Stomatology, Wuhan University, Wuhan, 430079, China; [2]Department of Oral and Maxillofacial-Head and Neck Oncology, School and Hospital of Stomatology, Wuhan University, Wuhan, 430079, China

Received February 8, 2015; Accepted April 12, 2015; Epub April 15, 2015; Published May 1, 2015

Abstract: In this study, we accessed the expression and correlation of p-STAT3 with Survivin, Cyclin D1, CD147, Slug and Ki67 by immunohistochemical staining of human tissue microarray which contains 72 adenoid cystic carcinoma (AdCC), 12 pleomorphic adenoma (PMA) and 18 normal salivary gland (NSG) using digital pathological scanner and scoring system. We found that the expression of p-STAT3, Survivin, Slug, Cyclin D1 and CD147 was significantly increased in AdCC as compared with PMA and (or) NSG ($p<0.05$). While, the level of p-STAT3 and expression of Cyclin D1 and CD147 was not associated with pathological type of human AdCC ($p>0.05$). Correlation analysis of these proteins revealed that p-STAT3 up-regulates the expression of Survivin, Slug, Cyclin D1 and CD147 ($p<0.05$). Moreover, the activation of STAT3 was associated with proliferation marker Ki-67 ($p<0.05$). Selective inhibition of STAT3 by a small molecule S3I-201 significantly reduced human SACC-83 and SACC-LM cells proliferation, migration and invasion with the corresponding decrease in expression of Survivin, Slug, Cyclin D1 and CD147. These findings indicate that high phosphorylation level of STAT3 in AdCC is related to Survivin, Slug, Cyclin D1 and CD147. We suggest that the inhibition of STAT3 may be a novel strategy for neoadjuvant chemotherapeutic treatment of AdCC.

Keywords: STAT3, Cyclin D1, CD147, adenoid cystic carcinoma, S3I-201

Introduction

Adenoid cystic carcinoma (AdCC) is one of the most frequent malignant salivary gland tumors in the head and neck region [1, 2]. It was characterized by a high rate of local recurrence, strong peripheral invasion and distant metastasis. Despite complete surgical resection and additional radiotherapy, the overall survival of AdCC has not been improved in the last three decades [1, 3]. To date, the molecular mechanism of the aggressive growth of AdCC remains unclear. Therefore, there is an urgent need to explore the molecular mechanism and novel drug target for AdCC.

STAT3, a gene has been mapped to chromosome 12, was activated to phosphorylation in response to extracellular ligands [4]. STAT3 has been recognized as an oncogene, it was expressed and activated in a variety of primary tumors, including head and neck squamous cell carcinoma [5]. STAT3 phosphorylation (p-STAT3), generally correlated with the active state, is a novel target for cancer treatment. Small molecule inhibitors including FLLL31, FLLL32, NSC74859 have shown the effects in cancer therapy such as breast cancer, pancreatic cancer and hepatoma [6]. Survivin has been identified as a key downstream target of STAT3 signaling [7], and over-expressed in a variety of cancer functions as a cell cycle regulator and inhibitor of apoptosis including AdCC [8]. Importantly, p-STAT3 and Survivin are attracting attention as novel cancer therapeutic targets in cancer [9, 10]. However, the mechanism underlying the effect of p-STAT3 and Survivin on the signaling transduction pathway which is activated in AdCC remains unclear.

Cyclin D1 mapping on the 11q13 is a nuclear protein that contributes to cell cycle progression and is a hallmark of many cancers which

contribute to tumor cell growth and cancer progression [11, 12]. Recent evidences have demonstrated that Slug has a crucial role in the cancer invasion and metastasis [13, 14]. We also have previously reported that Slug-mediated epithelial- mesenchymal transition plays an important role in the process of metastasis and apoptosis [15]. CD147 is a plasma membrane protein of Ig superfamily and promotes cancer cell invasion and metastasis through induction of MMPs production [16, 17].

In our study, we investigated the expression of p-STAT3, Survivin, Slug, Cyclin D1 and CD147 by tissue microarray in human AdCC. The correlation of p-STAT3 with Survivin, Slug, Cyclin D1 and CD147 and proliferation (Ki67) were analyzed in human AdCC. To investigate the role of these molecules in tumorigenesis, specifically in carcinogenesis of AdCC, we also studied the expression of these proteins in the AdCC along with common salivary gland benign tumor polymorphic adenoma (PMA) and normal salivary gland (NSG). Furthermore, we investigated the role of p-STAT3^{T705} in proliferation, migration and invasion of AdCC by target inhibition of STAT3 using small molecule S3I-201 *in vitro*.

Materials and methods

Chemical and reagents

All chemical and reagents were purchased from Sigma-Aldrich unless specified. S3I-201 was purchased from Selleck chemicals (Houston, TX). Primary antibody against human p-STAT3, Survivin, Slug and Ki-67 were purchased from Cell Signaling Technology (Danvers, MA), CD147 was purchased from Proteintech Group, Inc. (Chicago, IL).

Patients' specimens and ethics statement

All tissue samples of AdCC and PMA were obtained from the department of Oral and Maxillofacial-Head and Neck Oncology, School and Hospital of Stomatology, Wuhan University. For tissue microarray, we constructed a cohort including 72 AdCCs (cribriform pattern: 28, tubular pattern 24, solid pattern 20), 12 PMAs and 18 NSGs as previous described [18], in collaboration with Shanghai Biochip Company, Ltd, Shanghai, China (PI: Zhi-Jun Sun). All tumors were histology analyzed and classified according to the 2005 World Health Organization classification system. The study protocol was approved by Medical Ethics Committee of Hospital of Stomatology Wuhan University (PI: Zhi-Jun Sun). All subjects signed written informed consent.

Cell culture, drugs and cell immunofluorescence

SACC-83 and SACC-LM cell lines of human salivary AdCC were obtained from the China Center for Type Culture Collection, and were grown in Dulbecco's modified Eagle's medium (DMEM) supplemented with 10% FBS. The cells were incubated in a humidified atmosphere of 95% air and 5% CO_2 at 37°C. The following antibodies were used in this study: p-STAT3 (1:100), Cyclin D1 (1:100), Survivin (1:100), Slug (1:200) from Cell Signaling Technology, Inc., (Danvers, MA, USA), CD147 (1:100) from Proteintech Group, Inc. (Chicago, USA). S3I-201 was purchased from Selleck Chemicals, (Houston, TX, USA), and prepared in dimethyl sulfoxide (DMSO) as 200 mM stock solution stored at -20°C and used at a final concentration of 100 μM. SACC-83 or SACC-LM cells were seeded onto coverslips at a density of 10^5/mL and cultured in a 6-well plate for 24 hours with the indicated treatment. After treatment, cells were permeabilized in 0.2% Triton X-100 in PBS for 15 minutes, and blocked by non-immune goat serum for 60 minutes at room temperature. Then cells were incubated with primary antibody at dilutions recommended by the manufactures, after the PBS washout, PerCP-Cy5.5-conjugated secondary antibody (1:200. Jackson Immuno Research, USA) was used for detection and DAPI for nucleus counterstaining. Then the coverslips were mounted on microscope slides with antifade mounting media (Molecular Probes, Carlsbad, CA) and photographed with a fluorescence microscope (Leica).

Immunohistochemistry, scoring system, hierarchical clustering and date visualization

Immunohistochemistry for serial cut of human tissue microarray was performed as below described. All slides were rehydration and antigen retrieval using sodium citrate (pH=6.0) in a pressure cooker except p-STAT3 (EDTA buffer). Then the slides were treated in 3% hydrogen peroxide to block endogenous peroxidase activity and blocked with 2.5% bovine serum album

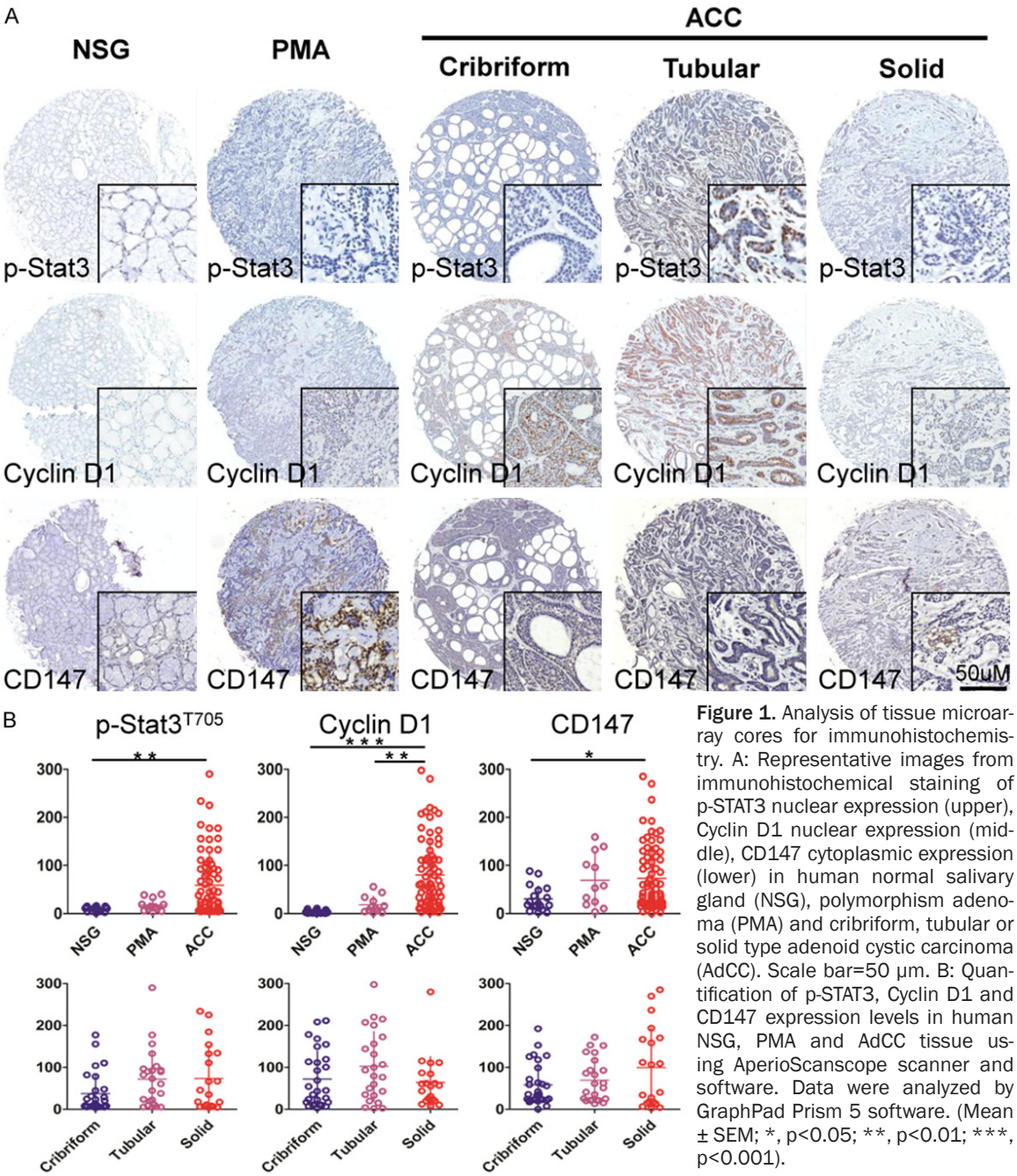

Figure 1. Analysis of tissue microarray cores for immunohistochemistry. A: Representative images from immunohistochemical staining of p-STAT3 nuclear expression (upper), Cyclin D1 nuclear expression (middle), CD147 cytoplasmic expression (lower) in human normal salivary gland (NSG), polymorphism adenoma (PMA) and cribriform, tubular or solid type adenoid cystic carcinoma (AdCC). Scale bar=50 μm. B: Quantification of p-STAT3, Cyclin D1 and CD147 expression levels in human NSG, PMA and AdCC tissue using AperioScanscope scanner and software. Data were analyzed by GraphPad Prism 5 software. (Mean ± SEM; *, $p<0.05$; **, $p<0.01$; ***, $p<0.001$).

in PBS buffer. Primary antibody were used with the following dilutions: p-STAT3 (1:200), Cyclin D1 (1:200), Survivin (1:200), Slug (1:200), CD147 (1:200), Ki-67 (1:400). Slides were incubated at 4°C overnight with indicated primary antibody and incubated with biotin-labeled secondary antibody and streptavidin peroxidase consequently, visualized by diaminobenzidine and counterstaining with hematoxylin. The immunohistochemical staining was scanned using an Aperio ScanScope CS whole slice scanner (Vista, CA, USA) with background subtraction. The positive result was quantified using Aperio Quantification software for membrane, nuclear, or pixel quantification and histoscore were calculated using formula (3+)×3+(2+)×2+(1+)×1 as previous described [19]. Immunohistochemical staining histoscore were converted into -3 to 3 using Microsoft Excel software, hierarchy clustering and visualization using Treeview were performed as previously described [20].

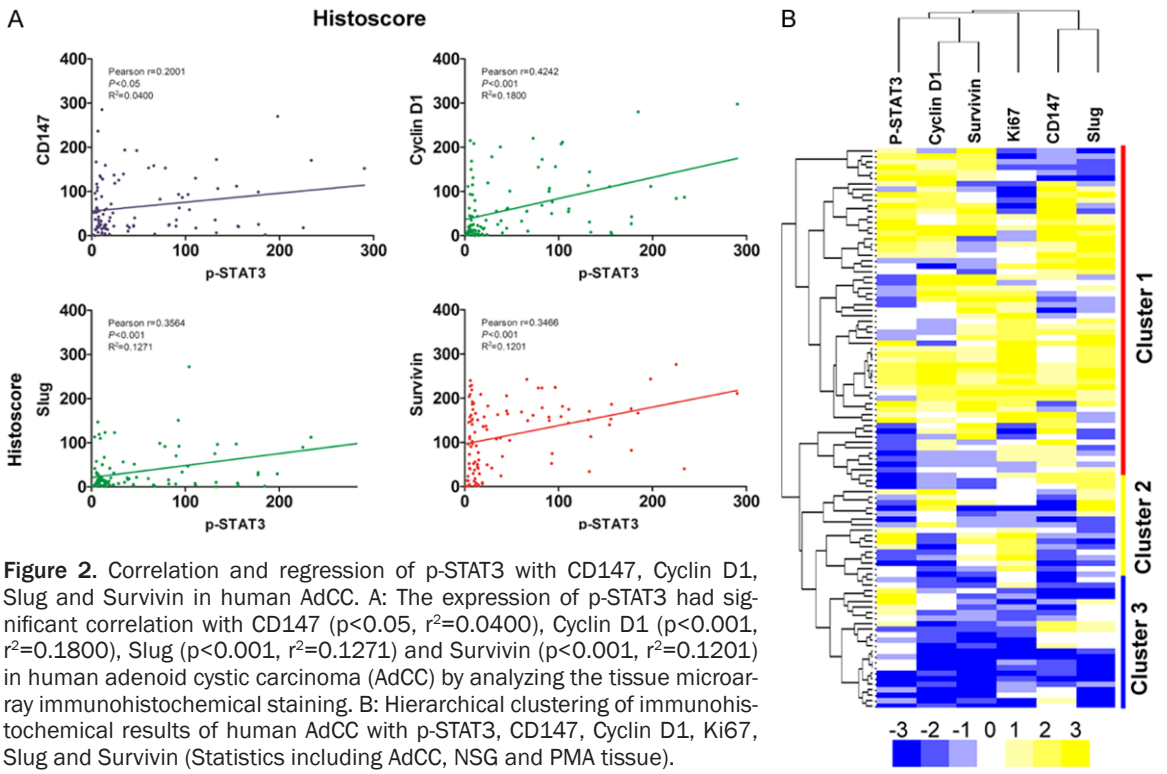

Figure 2. Correlation and regression of p-STAT3 with CD147, Cyclin D1, Slug and Survivin in human AdCC. A: The expression of p-STAT3 had significant correlation with CD147 ($p<0.05$, $r^2=0.0400$), Cyclin D1 ($p<0.001$, $r^2=0.1800$), Slug ($p<0.001$, $r^2=0.1271$) and Survivin ($p<0.001$, $r^2=0.1201$) in human adenoid cystic carcinoma (AdCC) by analyzing the tissue microarray immunohistochemical staining. B: Hierarchical clustering of immunohistochemical results of human AdCC with p-STAT3, CD147, Cyclin D1, Ki67, Slug and Survivin (Statistics including AdCC, NSG and PMA tissue).

Flow cytometry

Apoptosis was evaluated using Annexin V-fluorescein isothiocyanate methods. Following the same treatments as described for cell proliferation experiments, cells were washed with PBS, followed by lysis using trypsin (0.1%) and EDTA (0.01%) in PBS at pH 7.5. The cells were washed with normal media and cold PBS and resuspended in 1X binding buffer (BD-Pharmingen Biosciences, San Diego, CA). Then 5 ul Annexin and 5 ul propidium iodide (PI) were added to cells, which were vortexed and incubated for 15 minutes in the dark. Finally, 400 ul 1X binding buffer were added and samples evaluated by flow cytometry.

Western blotting

Total proteins were isolated from cultured SACC-83 or SACC-LM cells using M-PER (Pierce, Rockford, IL), and concentrations were detected by BCA assay kit (Pierce). Subsequently, 30 μg proteins from each sample were separated by 10% SDS-polyacrylamide gel and transferred electrophoretically to polyvinylidene difluoride (PVDF) membranes (Millipore, Bedford, MA). Membranes were blocked with 5% bovine serum albumin (BSA) in TBS containing 0.1% tween 20 (TBST) at room temperature for 60 minutes, then incubated overnight with primary antibody respectively at dilutions recommended by the manufactures. After fully incubation, bolts were detected by horseradish peroxidase-conjugated anti-mouse or anti-rabbit secondary antibody, and visualized with the Super-Signal West Femto maximum sensitivity substrate (Thermo Scientific, Rockford, IL, USA) on X-ray film. The images on X-ray films were then converted to electronic format using digital Scanner System (CanoScan LiDE110) and the density was calculated with Image J software packages.

Wound healing assay

SACC-83 or SACC-LM cells were seeded in 6-well plates (Corning Life Sciences, USA) at 1.0×10^5 cells/well. When cells reached 80% confluence, the center of each well was scratched with a sterile pipette tip to generate a constant gap, and then the cells were continued incubated with medium containing no FBS to 18 hours. After fixation cells were photographed under phase microscopy and counted as previously described.

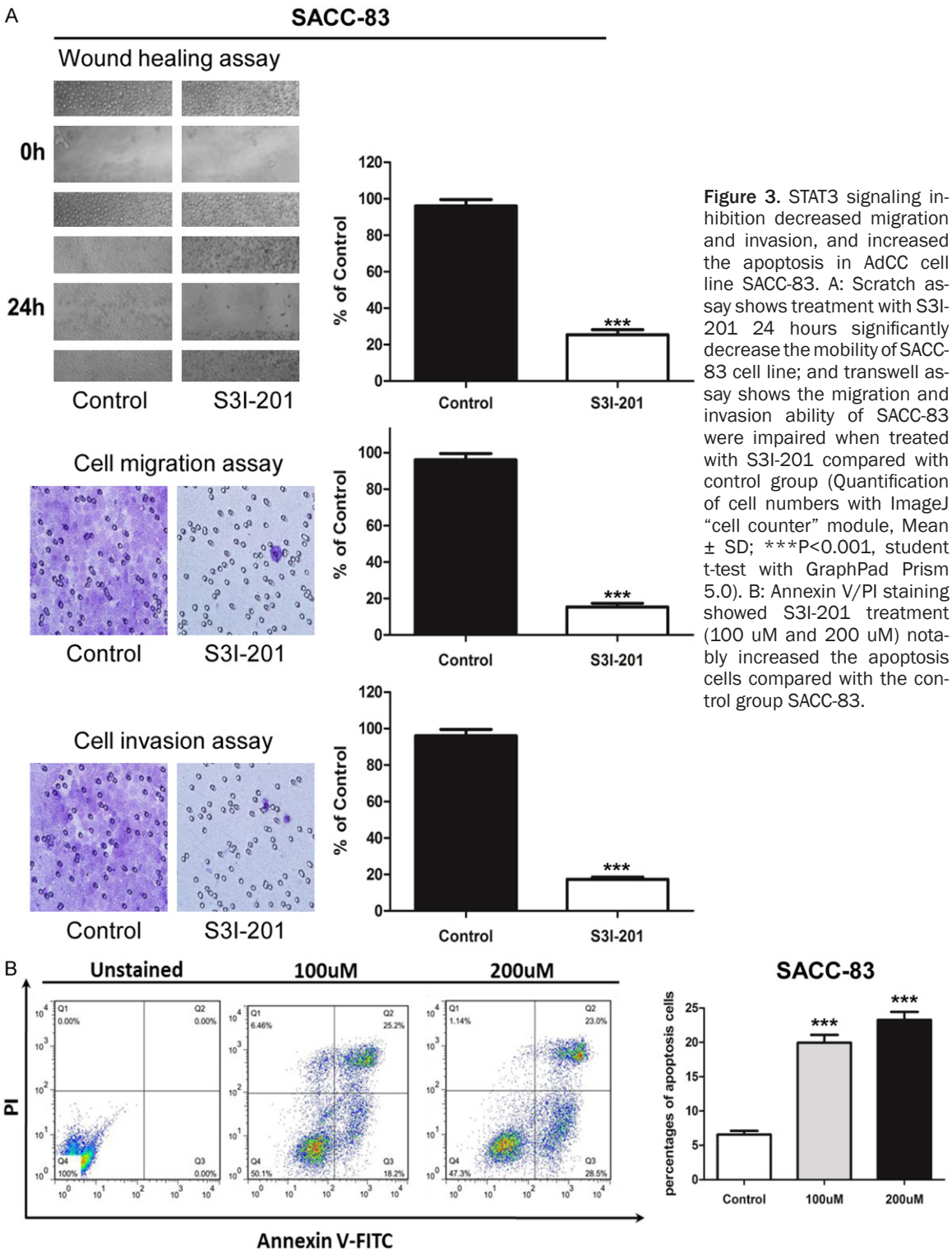

Figure 3. STAT3 signaling inhibition decreased migration and invasion, and increased the apoptosis in AdCC cell line SACC-83. A: Scratch assay shows treatment with S3I-201 24 hours significantly decrease the mobility of SACC-83 cell line; and transwell assay shows the migration and invasion ability of SACC-83 were impaired when treated with S3I-201 compared with control group (Quantification of cell numbers with ImageJ "cell counter" module, Mean ± SD; ***P<0.001, student t-test with GraphPad Prism 5.0). B: Annexin V/PI staining showed S3I-201 treatment (100 uM and 200 uM) notably increased the apoptosis cells compared with the control group SACC-83.

Transwell invasion assays

In vitro invasion assay was performed using Costar Transwell inserts (#3422, pore size, 8 μm) (Corning, Albany, NY) as described previously [21]. SACC-83 or SACC-LM cells were seeded into the upper chamber coated with Matrigel (BD Biosciences) at a density of 10^4/well in 100 ul serum-free medium, while 10% FBS medium was added to the bottom chamber to stimulate invasion. After incubation for 24 h at 37°C, the cells in the upper chamber

were carefully removed with cotton swab and the cells that had invaded through Matrigel were stained with crystal violet, and then photographed and quantified. Each assay was conducted in triplicate.

Statistical analysis

Statistical data analysis was performed with GraphPad Prism 5.01 (GraphPad Software, Inc., La Jolla, CA) statistical packages. The Mann-Whitney U test and student t test was used to evaluate differences in the Western blotting and immunofluorescence analysis. The One-way ANOVA followed by the post-Turkey or Bonferroni multiple comparison tests was used to analyze the differences in immunohistostaining. Two-tailed Pearson correlation was used for correlated expression of these markers after confirmation of the sample with a Gaussian distribution. $P<0.05$ was considered statistically significant.

Results

Immunohistochemical staining of p-STAT3, Cyclin D1, CD147, Slug, Survivin and Ki67 in human AdCC

We assessed the expression of p-STAT3, Cyclin D1, CD147, Slug, Survivin and Ki67 using human tissue microarray containing 72 AdCC, 12 PMA and 18 NSG. The positive expression of p-STAT3, Cyclin D1, Slug, Survivin and Ki67 was mainly located in nucleus of tumor cells. Whereas, CD147 was located in cytoplasm and/or cytomembrane (**Figure 1A** and Figure S1A). We found that weak expression of p-STAT3, Cyclin D1, Slug, Survivin and Ki67 in nuclear was inspected from NSG and PMA, but strongly expressed was tested in cribriform, tubular and solid histological patterns in human adenoid cystic carcinoma (**Figure 1A** and Figure S1A). CD147 was weak expression in cytoplasm and cytomembrane in NSG and PMA, but strongly expressed in AdCC (**Figure 1A**). To credibly illustrate high expression of p-STAT3, Cyclin D1, CD147, Slug, Survivin and Ki67 in human AdCC, we quantified the immunohistochemical stain of whole slide by Aperio ScanScope CS scanner (Vista, CA, USA). Nuclear analysis of p-STAT3, Cyclin D1, Slug, Survivin and Ki67 and membrane analysis of CD147 were calculated with Aperio nuclear count software (Version 1.0) and membrane count software (Version 1.0). Cytoplasm CD147 expression was calculated using Aperio positive pixel count software (Version 9.1). We found that AdCC cells showed significant staining for p-STAT3 as compared with NSG ($p<0.001$). PMA cells also showed no significant staining for p-STAT3 as compared with NSG ($p>0.05$, **Figure 1B**). For Cyclin D1, AdCC cells showed significant staining as compared with PMA and NSG ($p<0.01$, $p<0.001$, respectively, **Figure 1B**). For CD147, however, there was mildly increase in AdCC as compared with NSG to reach a statistic significant ($p<0.05$, **Figure 1B**). Slug, Survivin and Ki67 was highly expressed in AdCC tissues as compared with NSG ($p<0.001$ for Slug, $p<0.001$ for Survivin and $p<0.01$ for Ki67 respectively) and PMA ($p<0.001$ for Slug, $p<0.001$ for Survivin and $p>0.05$ respectively, Figure S1B). Taken together, the expression of p-STAT3, Cyclin D1, CD147, Slug, Survivin and Ki67 was significantly increased in AdCC as compared with NSG. To further determine whether the expression of p-STAT3, Cyclin D1, CD147, Slug, Survivin associates with histopathology pattern of AdCC, we analyzed these makers expression in cribriform, tubular and solid form of AdCC. While, the three patterns of AdCC have no statistics significance in p-STAT3, Cyclin D1, CD147, expression (**Figure 1B**).

The correlation between p-STAT3 and Cyclin D1, CD147, Slug, Survivin and Ki67 in human NSG, PMA and AdCC

To evaluate the association of p-STAT3 signaling pathway with Cyclin D1, CD147, Slug, Survivin and Ki67 in human NSG, PMA and AdCC, we analyzed the quantitative outcome of immunohistochemical staining by the Spearman rank correlation coefficient test and linear tendency test. The result demonstrates that the expression of p-STAT3 had significant correlation with CD147 ($p<0.05$, $r^2=0.0400$), Cyclin D1 ($p<0.001$, $r^2=0.1800$), Slug ($p<0.001$, $r^2=0.1271$), Survivin ($p<0.001$, $r^2=0.1201$) and Ki67 ($p<0.001$, $r^2=0.1313$), meanwhile linear regression indicated the positive trendline between p-STAT3 with Cyclin D1, CD147, Slug, Survivin and Ki67 (**Figure 2A**, Figure S1B, S1C). By clustering, these relationships in human AdCC was displayed in a visual image (**Figure 2B**), and Cyclin D1/Survivin and CD147/Slug has close correlation with p-STAT3. Of interest, using hierarchical clustering analysis, most of the AdCC cases (cluster 1) were distinct from

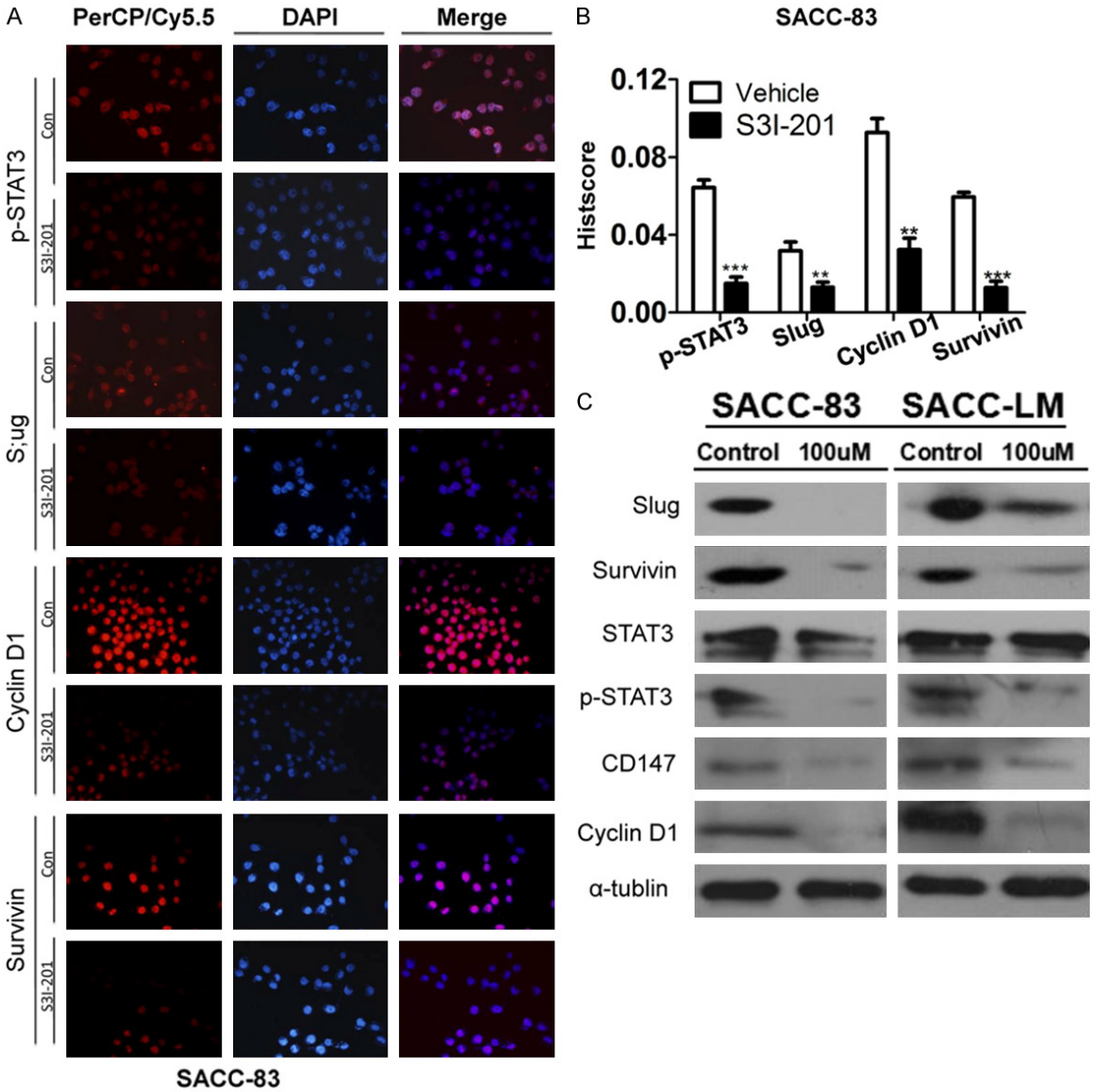

Figure 4. S3I-201 treatment inhibits the STAT3 signaling pathway. A: Immunofluorescence shows treatment with S3I-201 24 hours decrease the expression of p-STAT3, Cyclin D1, Slug and Survivin in SACC-83 cell line. B: Quantification of immunofluorescence for SACC-83 with Image J, IOD for mean integrated optical density and calculated with total optical density divided by the area. C: Western blot shows that S3I-201 decrease the expression of p-STAT3, CD147, Cyclin D1, Ki67, Slug and Survivin in SACC-83 and SACC-LM cells.

PMA (cluster 2) and NSG (cluster 3), reflecting the significant differences in p-STAT3, Cyclin D1, CD147, Slug and Survivin staining in AdCC.

STAT3 signaling inhibition with S3I-201 decrease AdCC migration and invasion

To determine whether STAT3 blockade decrease the malignancy of AdCC, we performed *in vitro* inhibition assay of S3I-201, a putative STAT3 inhibitor on SACC-83 and SACC-LM cell lines, wound healing and Boyden chamber invasion assay were carried out to detect the migration and invasion potential. As showed in **Figure 3A**, p-STAT3 inhibition dramatically decreased the migration behavior and the cell number of migration was clearly different between control and S3I-201 treatment group ($p<0.001$). We then examined the invasion ability change after S3I-201 inhibition with the Boyden chamber assay. The results showed S3I-201 treatment notably decreased the invasion cells compared

with the control group in SACC-83 (**Figure 3A**), similar results were observed in SACC-LM (Figure S2A).

S3I-201 induces apoptosis in SACC-83 and SACC-LM cell lines

To determine whether the decrease in cell survival was mediated by induction of apoptosis, we analyzed the effect of 100 μM S3I-201 on SACC-83 and SACC-LM using flow cytometry. The results of Annexin V/PI staining showed S3I-201 treatment notably increased the apoptosis cells compared with the control group in SACC-83 ($P<0.001$, **Figure 3B**), similar results were observed in SACC-LM (Figure S2B).

S3I-201 suppress the expression of p-STAT3, Cyclin D1, CD147, survivin and Slug in human SACC-83 and SACC-LM cell lines

Base on the observation that expression of p-STAT3 correlated with Cyclin D1, CD147, Survivin and Slug staining in AdCC. We direct investigated the effect of STAT3 inhibition in human AdCC cell lines. Western blot results revealed expression of p-STAT3, Cyclin D1, CD147, Survivin and Slug were significantly suppressed when SACC-83 cells were treated with 100 μM S3I-201 as compared with control group (**Figure 4C**). Immunofluorescence revealed that S3I-201 significantly decrease p-STAT3, Slug, Cyclin D1 and Survivin nuclear expression (**Figure 4A** with quantification in **Figure 4B**). Similar results were observed in SACC-LM (Figure S2A and S2B).

Discussion

In the present study, we investigated potential correlation of p-STAT3 and Cyclin D1, CD147, Slug, Survivin and Ki67 pathway to reveal mechanisms on STAT3 related proliferation, apoptosis and invasion. We initially found that p-STAT3 and Cyclin D1, CD147, Slug, Survivin were highly expressed in AdCC as compared with PMA or NSG. Moreover, p-STAT3 could mediate the expression of Cyclin D1, CD147, Slug, Survivin and Ki67, suggesting high expression p-STAT3 promoted tumor proliferation and invasion. Furthermore, *in vitro* experiment directly observed that STAT3 inhibitor S3I-201 decreased the expression of p-STAT3 and Cyclin D1, CD147, Slug, Survivin as compared with the control group in SACC-83 and SACC-LM, indicating that STAT3 inhibition may be a novel strategy for neoadjuvant chemotherapeutic treatment of AdCC.

Firstly, p-STAT3 and Cyclin D1, CD147, Slug, Survivin were highly expressed in AdCC as compared with NSG in this study. As we known, p-STAT3 and Cyclin D1, CD147, Slug, Survivin were over-expressed in a variety of cancer, including head and neck cancer, lung cancer and hepatoma cancer [5, 11, 16]. We found that AdCC cells showed significant staining for p-STAT3 as compared with NSG. The expression of Cyclin D1 was significantly higher in AdCC when compared with PMA and/or NSG. The expression of Slug, Survivin and Ki67 were highly expressed in AdCC tissues as compared with NSG and PMA. We further investigated the role of these markers in the differential diagnosis of the pathological type of AdCC because several studies have identified pathological factors in AdCC with an unfavorable effect on survival. In hepatocellular carcinoma, p-STAT3 was correlated with large tumor size, frequent intrahepatic metastasis, poor prognosis and high recurrence rate [22]. However, our present data showed the expression of p-STAT3, cyclin D1, and CD147 did not reach statistical significance in three pathological type of AdCC. Of interest, hierarchical clustering analysis showed that most of the AdCC cases were distinct from PMA and NSG, reflecting the significant differences in p-STAT3, Cyclin D1, CD147, Slug and Survivin staining in AdCC.

STAT3 has been detected in a wide variety of human cancers and is believed to be one of the important factors for cancer proliferation, invasion, metastasis and epithelial- mesenchymal transition [9, 23]. In human prostate cancer, the expression of cyclin D1 and Survivin were inhibited after the phosphorylation of STAT3 was inhibited by ginkgetin [24]. However, the role of STAT3 activation in the development of AdCC has not been well understood. Our results showed that p-STAT3 was statistically associated with CD147, Cyclin D1, Slug, Survivin and Ki67. Recently, a report showed that cancer cell migration and angiogenesis could be inhibit when the STAT3 constitutive phosphorylation was inhibited by LY5, and the expression of cyclin D1, Bcl-XL, Survivin, and microRNA-21 were down-regulated in the Medulloblastoma cells [25]. p-STAT3 was correlated with α-fetoprotein, Ki-67 and Bcl-XL in hepatocellular car-

cinoma [22]. However, the molecular mechanisms of p-STAT3 and Cyclin D1, CD147, Slug, Survivin have not been investigated in AdCC.

Up to now, S3I-201 or its homologs were testified to be a potent therapeutic agent for some such highly malignant disease as hepatocellular carcinoma, esophageal cancer and non-small cell lung cancer [26-28]. Molecular mechanism study indicate that S3I-201 act on p-STAT3 to inhibit STAT3 signaling pathway [25]. Our data showed that the migration and invasion potential were inhibited when the SACC-83 and SACC-LM cell lines were treated with S3I-201. A new report showed that STAT3-induced miR-92a promotes cancer invasion by suppressing RECK in lung cancer [29], which was insistent with our results and suggesting that STAT3 was a potential target for the cancer treatment. Our results also showed S3I-201 treatment notably increased apoptosis in SACC-83 and SACC-LM cell lines, and the expression of p-STAT3 and Cyclin D1, CD147, Slug and Survivin were inhibited after the cancer cells were treated with S3I-201. In osteosarcoma, STAT3 phosphorylation and downstream STAT3-target genes Cyclin D1 and Survivin were down-regulated, the osteosarcoma cell growth was suppressed and apoptosis was induced [30]. In addition, we also have previously reported that Slug-mediated epithelial-mesenchymal transition -like transformation plays an important role in the process of metastasis and apoptosis [15]. S3I-201 could inhibit STAT3 activity and suppressed doxorubicin-induced epithelial- mesenchymal transition in hepatocellular carcinoma [26]. All these researches indicated that STAT3 targeted-therapy may have therapeutic potential in AdCC, and S3I-201 may be a potential therapeutic agent for human cancer cells expressing constitutive STAT3 signaling.

In conclusion, our results has confirmed the important roles of p-STAT3 signaling is up-regulated in the AdCC and may be involved in tumor progression through interaction with cyclin D1, CD147 and Survivin. Our work has also revealed that p-STAT3 signaling promotes invasion and metastasis of AdCC conspired with Slug, CD147 program in AdCC cell lines. Thus, targeting STAT3 signaling may be a potential candidate for treatment of AdCC.

Acknowledgements

This work was supported by National Natural Science Foundation of China (81072203, 81272963, 81472528) to Z.J. Sun, (81272946, 81472529) to W.F. Zhang and (81402241) to C.F. Huang. This work was also supported by program for new century excellent talents in university (NCET-13-0439), Ministry of Education of China to Z.J. Sun.

Disclosure of conflict of interest

The authors have declared that no competing interests exist.

Abbreviations

AdCC, adenoid cystic carcinoma; PMA, pleomorphic adenoma; NSG, normal salivary gland; STAT3, signal transducer and activator of transcription 3.

Address correspondence to: Zhi-Jun Sun or Wen-Feng Zhang, The State Key Laboratory Breeding Base of Basic Science of Stomatology & Key Laboratory of Oral Biomedicine Ministry of Education, Department of Oral and Maxillofacial-Head and Neck Oncology, School and Hospital of Stomatology, Wuhan University, Wuhan, China. Tel: 86-27-87686108; Fax: 86-27-87873260; E-mail: zhijundejia@163.com (ZJS); zhangwf59@163.com (WFZ)

References

[1] Sun ZJ, Chen G, Zhang W, Hu X, Huang CF, Wang YF, Jia J and Zhao YF. Mammalian target of rapamycin pathway promotes tumor-induced angiogenesis in adenoid cystic carcinoma: its suppression by isoliquiritigenin through dual activation of c-Jun NH2-terminal kinase and inhibition of extracellular signal-regulated kinase. J Pharmacol Exp Ther 2010; 334: 500-512.

[2] Patel KJ, Pambuccian SE, Ondrey FG, Adams GL and Gaffney PM. Genes associated with early development, apoptosis and cell cycle regulation define a gene expression profile of adenoid cystic carcinoma. Oral Oncol 2006; 42: 994-1004.

[3] Frierson HF Jr, El-Naggar AK, Welsh JB, Sapinoso LM, Su AI, Cheng J, Saku T, Moskaluk CA and Hampton GM. Large scale molecular analysis identifies genes with altered expression in salivary adenoid cystic carcinoma. Am J Pathol 2002; 161: 1315-1323.

[4] Darnell JE Jr. Reflections on STAT3, STAT5, and STAT6 as fat STATs. Proc Natl Acad Sci U S A 1996; 93: 6221-6224.
[5] Kijima T, Niwa H, Steinman RA, Drenning SD, Gooding WE, Wentzel AL, Xi S and Grandis JR. STAT3 activation abrogates growth factor dependence and contributes to head and neck squamous cell carcinoma tumor growth in vivo. Cell Growth Differ 2002; 13: 355-362.
[6] Lin L, Hutzen B, Zuo M, Ball S, Deangelis S, Foust E, Pandit B, Ihnat MA, Shenoy SS, Kulp S, Li PK, Li C, Fuchs J and Lin J. Novel STAT3 phosphorylation inhibitors exhibit potent growth-suppressive activity in pancreatic and breast cancer cells. Cancer Res 2010; 70: 2445-2454.
[7] Lin L, Amin R, Gallicano GI, Glasgow E, Jogunoori W, Jessup JM, Zasloff M, Marshall JL, Shetty K, Johnson L, Mishra L and He AR. The STAT3 inhibitor NSC 74859 is effective in hepatocellular cancers with disrupted TGF-beta signaling. Oncogene 2009; 28: 961-972.
[8] Liao Y, Zeng H, Wang X, Huang Y, Chen N, Ge B, Tang L and Luo Q. Expression patterns and prognostic significance of inhibitor of apoptosis proteins in adenoid cystic carcinoma and pleomorphic adenoma of lachrymal gland. Exp Eye Res 2009; 88: 4-11.
[9] Yu H, Lee H, Herrmann A, Buettner R and Jove R. Revisiting STAT3 signalling in cancer: new and unexpected biological functions. Nat Rev Cancer 2014; 14: 736-746.
[10] Huang J, Lyu H, Wang J and Liu B. MicroRNA regulation and therapeutic targeting of survivin in cancer. Am J Cancer Res 2015; 5: 20-31.
[11] Pestell RG. New roles of cyclin D1. Am J Pathol 2013; 183: 3-9.
[12] Zhou CX and Gao Y. Aberrant expression of beta-catenin, Pin1 and cylin D1 in salivary adenoid cystic carcinoma: relation to tumor proliferation and metastasis. Oncol Rep 2006; 16: 505-511.
[13] Choi MJ, Cho KH, Lee S, Bae YJ, Jeong KJ, Rha SY, Choi EJ, Park JH, Kim JM, Lee JS, Mills GB and Lee HY. hTERT mediates norepinephrine-induced Slug expression and ovarian cancer aggressiveness. Oncogene 2014.
[14] Li Y, Zhao Z, Xu C, Zhou Z, Zhu Z and You T. HMGA2 induces transcription factor Slug expression to promote epithelial-to-mesenchymal transition and contributes to colon cancer progression. Cancer Lett 2014; 355: 130-140.
[15] Zhao ZL, Ma SR, Wang WM, Huang CF, Yu GT, Wu TF, Bu LL, Wang YF, Zhao YF, Zhang WF, Sun ZJ. Notch signaling induces epithelial-mesenchymal transition to promote invasion and metastasis in adenoid cystic carcinoma. Am J Transl Res 2015; 7: 162-174.
[16] Huang C, Sun Z, Sun Y, Chen X, Zhu X, Fan C, Liu B, Zhao Y and Zhang W. Association of increased ligand cyclophilin A and receptor CD147 with hypoxia, angiogenesis, metastasis and prognosis of tongue squamous cell carcinoma. Histopathology 2012; 60: 793-803.
[17] Wang SJ, Cui HY, Liu YM, Zhao P, Zhang Y, Fu ZG, Chen ZN and Jiang JL. CD147 promotes Src-dependent activation of Rac1 signaling through STAT3/DOCK8 during the motility of hepatocellular carcinoma cells. Oncotarget 2015; 6: 243-257.
[18] Yu GT, Bu LL, Zhao YY, Liu B, Zhang WF, Zhao YF, Zhang L and Sun ZJ. Inhibition of mTOR reduce Stat3 and PAI related angiogenesis in salivary gland adenoid cystic carcinoma. Am J Cancer Res 2014; 4: 764-775.
[19] Wang YF, Ma SR, Wang WM, Huang CF, Zhao ZL, Liu B, Zhang WF, Zhao YF, Zhang L and Sun ZJ. Inhibition of survivin reduces HIF-1alpha, TGF-beta1 and TFE3 in salivary adenoid cystic carcinoma. PLoS One 2014; 9: e114051.
[20] Wang YF, Zhang W, He KF, Liu B, Zhang L, Zhang WF, Kulkarni AB, Zhao YF and Sun ZJ. Induction of autophagy-dependent cell death by the survivin suppressant YM155 in salivary adenoid cystic carcinoma. Apoptosis 2014; 19: 748-758.
[21] Zhang L, Sun ZJ, Bian Y and Kulkarni AB. MicroRNA-135b acts as a tumor promoter by targeting the hypoxia-inducible factor pathway in genetically defined mouse model of head and neck squamous cell carcinoma. Cancer Lett 2013; 331: 230-238.
[22] Mano Y, Aishima S, Fujita N, Tanaka Y, Kubo Y, Motomura T, Taketomi A, Shirabe K, Maehara Y and Oda Y. Tumor-associated macrophage promotes tumor progression via STAT3 signaling in hepatocellular carcinoma. Pathobiology 2013; 80: 146-154.
[23] Wendt MK, Balanis N, Carlin CR and Schiemann WP. STAT3 and epithelial-mesenchymal transitions in carcinomas. JAKSTAT 2014; 3: e28975.
[24] Jeon YJ, Jung SN, Yun J, Lee CW, Choi J, Lee YJ, Han DC and Kwon BM. Ginkgetin inhibits the growth of DU-145 prostate cancer cells through inhibition of STAT3 activity. Cancer Sci 2015; 106: 413-20.
[25] Xiao H, Bid HK, Jou D, Wu X, Yu W, Li C, Houghton PJ and Lin J. A Novel Small Molecular STAT3 Inhibitor, LY5 Inhibits Cell Viability, Cell Migration, And Angiogenesis in Medulloblastoma Cells. J Biol Chem 2015; 290: 3418-29.
[26] Hu QD, Chen W, Yan TL, Ma T, Chen CL, Liang C, Zhang Q, Xia XF, Liu H, Zhi X, Zheng XX, Bai XL, Yu XZ and Liang TB. NSC 74859 enhances doxorubicin cytotoxicity via inhibition of epithe-

lial-mesenchymal transition in hepatocellular carcinoma cells. Cancer Lett 2012; 325: 207-213.

[27] Zhang C, Yang X, Zhang Q, Guo Q, He J, Qin Q, Zhu H, Liu J, Zhan L, Lu J, Liu Z, Xu L, Ma J, Dai S, Cheng H and Sun X. STAT3 inhibitor NSC74859 radiosensitizes esophageal cancer via the downregulation of HIF-1alpha. Tumour Biol 2014; 35: 9793-9799.

[28] Jin HO, Lee YH, Park JA, Kim JH, Hong SE, Kim HA, Kim EK, Noh WC, Kim BH, Ye SK, Chang YH, Hong SI, Hong YJ, Park IC and Lee JK. Blockage of Stat3 enhances the sensitivity of NSCLC cells to PI3K/mTOR inhibition. Biochem Biophys Res Commun 2014; 444: 502-508.

[29] Lin HY, Chiang CH and Hung WC. STAT3 upregulates miR-92a to inhibit RECK expression and to promote invasiveness of lung cancer cells. Br J Cancer 2013; 109: 731-738.

[30] Wang X, Goldstein D, Crowe PJ and Yang JL. Impact of STAT3 inhibition on survival of osteosarcoma cell lines. Anticancer Res 2014; 34: 6537-6545.

A

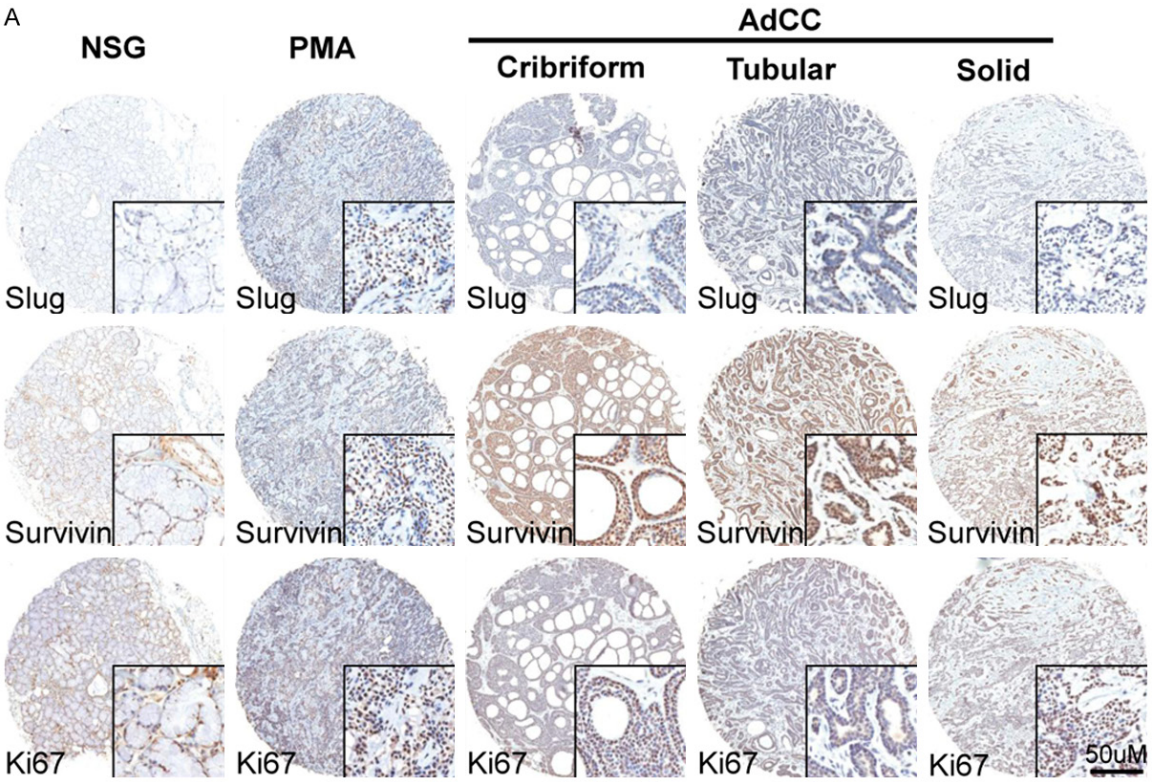

B

Marker	NSG vs PMA	NSG vs AdCC	PMA vs AdCC
Slug	<0.001	<0.001	<0.001
Survivin	>0.05	<0.001	<0.001
Ki67	>0.05	<0.01	>0.05

C

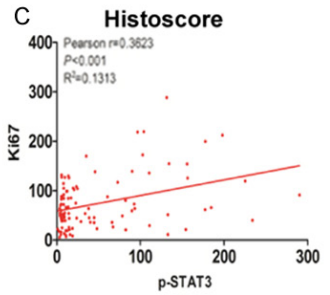

Figure S1. Analysis of tissue microarray cores for immunohistochemistry. A: Representative images from immunohistochemical staining of Slug (upper)and Ki67 (lower) nuclear expression, Survivin nuclear and cytoplasmic expression (middle) in human normal salivary gland (NSG), polymorphism adenoma (PMA) and cribriform, tubular or solid type adenoid cystic carcinoma (AdCC). Scale bar=50 μm. B: Quantification of Slug, Survivin and Ki67 expression levels in human NSG, PMA and AdCC tissue using AperioScanscope scanner and software. C: The expression of p-STAT3 had significant correlation with Ki67 ($p<0.001$, $r^2=0.1313$). Data were analyzed by GraphPad Prism 5 software. (Mean ± SEM; *, $p<0.05$; **, $p<0.01$; ***, $p<0.001$).

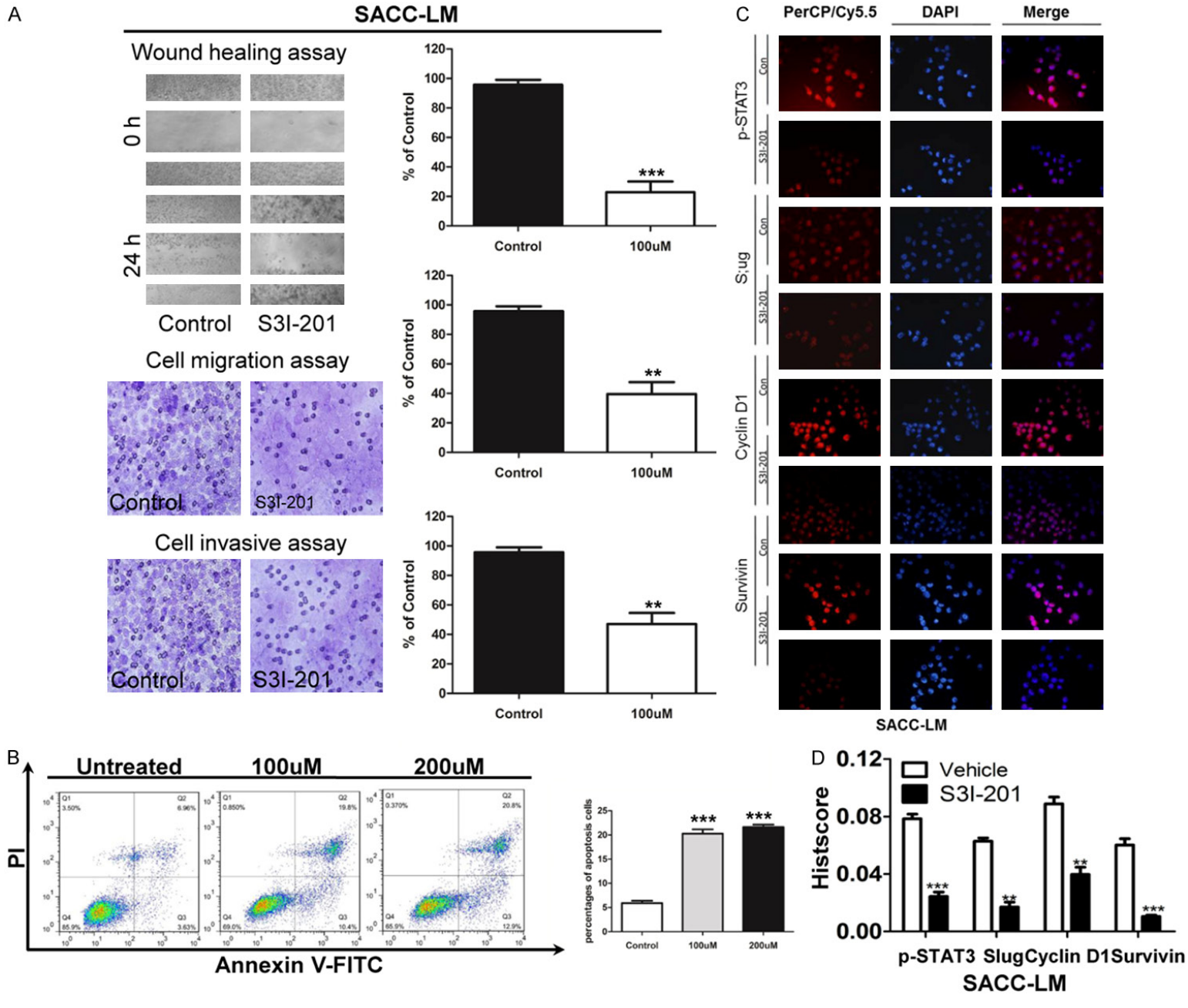
A
SACC-LM
Wound healing assay
0 h
24 h
Control
S3I-201
Cell migration assay
Control
S3I-201
Cell invasive assay
Control
S3I-201
% of Control
Control
100uM
***
**
**
C
PerCP/Cy5.5
DAPI
Merge
p-STAT3
S;ug
Cyclin D1
Survivin
Con
S3I-201
SACC-LM
B
Untreated
100uM
200uM
PI
Annexin V-FITC
percentages of apoptosis cells
Control
100uM
200uM
D
Vehicle
S3I-201
Histscore
p-STAT3
Slug
Cyclin D1
Survivin
SACC-LM

Figure S2. STAT3 signaling inhibition decreased migration and invasion, and increased the apoptosis in AdCC cell line SACC-LM. A: Scratch assay shows treatment with S3I-201 24 hours significantly decrease the mobility of SACC-LM cell line; and transwell assay shows the migration and invasion ability of SACC-83 were impaired when treated with S3I-201 compared with control group (Quantification of cell numbers with ImageJ "cell counter" module, Mean ± SD; ***P<0.001, student t-test with GraphPad Prism5.0). B: Annexin V/PI staining showed S3I-201 treatment (100 uM and 200 uM) notably increased the apoptosis cells compared with the control group SACC-LM. C: Immunofluorescence shows treatment with S3I-201 24 hours decrease the expression of p-STAT3, Cyclin D1, Slug and Survivin in SACC-LM cell line. D: Quantification of immunofluorescence for SACC-LM with Image J, IOD for mean integrated optical density and calculated with total optical density divided by the area.